Design and performance evaluation of spheroid geometry for brain PET scanner using Monte Carlo modeling

Original Article

Peyman Sheikhzadeh[1,2], Hossein Ghadiri[1,2], Parham Geramifar[3], Pardis Ghafarian[4,5], Mohammad Reza Ay[1,2]

[1]Department of Medical Physics and Biomedical Engineering, Tehran University of Medical Science, Tehran Iran
[2]Research Center for Molecular and Cellular Imaging, Tehran University of Medical Sciences, Tehran, Iran
[3]Research Center for Nuclear Medicine, Tehran University of Medical Sciences, Tehran, Iran
[4]Chronic Respiratory Diseases Research Center, National Research Institute of Tuberculosis and Lung Diseases, Shahid Beheshti University of Medical Sciences, Tehran, Iran
[5]PET/CT and Cyclotron Center, Masih Daneshvari Hospital, Shahid Beheshti University of Medical Sciences, Tehran, Iran

(Received 17 October 2017, Revised 11 November 2018, Accepted 13 November 2018)

ABSTRACT

Introduction: There has been a curiosity about the spheroid geometry for PET scanners developments since several years ago, therefore in this study, we are aiming to evaluate the performance of this geometry and compare its performance with cylindrical geometry using Monte Carlo simulation.

Methods: We simulated a spheroid geometry with a radius of 199 mm, patient bore with of radius of 175 mm, which is compatible with brain size. In second design, cylindrical geometry was simulated with transaxial FOV and ring radius of 175 mm as well. Photon detection efficiency (PDE), NEMA line source sensitivity, spatial resolution and Derenzo phantom image quality were analyzed.

Results: We obtained PDE about 21.7% versus 23.8% in 250-750 keV and 19.5% versus 21.3% in 410-613 keV for point source in center of FOV for spheroid and cylindrical PET respectively. The results of NEMA sensitivity measurements indicate 3.29 kcps/MBq versus 3.64 kcps/MBq for spheroid and cylindrical designs. The spatial resolution (FWHM) calculations using MLEM reconstruction algorithm show around 1.6 mm for transvers and axial resolution for point source placed in center of FOV for both scanners. Also we found for spheroid and cylindrical designs 4.8 and 2.7 mm versus 4 and 3.6 mm as transvers and axial mean resolution for off-center point sources.

Conclusion: Performance evaluation study indicates that the spheroid geometry delivers better axial resolution whereas cylindrical design can still provide higher sensitivity and transvers spatial resolution than the spheroid geometry PET with same scanner bore size.

Key words: PET; Spheroid design; Spatial resolution; Monte Carlo; Simulation

Iran J Nucl Med 2019;27(1):32-38
Published: January, 2019
http://irjnm.tums.ac.ir

Corresponding author: Dr. Mohammad Reza. Ay, Department of Medical Physics and Biomedical Engineering, Tehran University of Medical Sciences, Tehran, Iran. E-mail: mohammadreza_ay tums.ac.ir

INTRODUCTION

In the most recent years, dedicated positron emission tomography (PET) scanners have been developed with a rapid growth aiming to improve sensitivity and spatial resolution over conventional whole-body PET scanner for accurate brain [1-4] and breast [5, 6] imaging. Compared to conventional whole body PET scanners, these types of scanners, can serve increased system sensitivity due to small field of view (FOV) at lower cost [7]. System sensitivity is mainly affected by the scanner geometry and detector specifications [2, 8]. There has been proposed different scanner geometry for increase the solid angle coverage and subsequently improve geometrical sensitivity such as box shape and spheroid design and etc. [8-12].

One of the first symmetrical spheroid designs was proposed by Ficke et al. as they proposed spheroid PET with six rings of trapezoid shaped block detector [9]. This scanner demands different polygonal shape detectors, leading to more manufacturing complexity along with increased costs. Moreover, a non-symmetrical spherical (hemispherical) designs has been recently presented similar to helmet geometry [13]. As overall hemispherical designs incompletely cover line of responses (LOR) so many data missing, these non-symmetrical designs needs additional detector to detect some of these missed LOR's [13]. Such designs increase depth of interaction (DOI) error (parallax error) in peripheral LOR's, degrading quantification in regions of interest [2].

Symmetric spheroid design in addition to brain dedicated PET is a suitable candidate for breast and even whole-body scanners. There has been considerable interest about the spheroid geometry for PET scanners developments from the several years ago, therefore in this study, we are aiming to evaluate this geometry based on conventional square block detectors. We use Monte Carlo simulation as a powerful, accurate and useful tools for scanner design and performance evaluation. For comparative assessment with cylindrical geometry some parameters such as detection efficiency, NEMA sensitivity and spatial resolution were calculated using MC simulation.

METHODS

Scanner modeling

We simulated two geometries: First, a spheroid geometry with a radius of 199 mm, patient bore with radius of 175 mm, which is compatible with brain size. The system contains 3 detector rings, providing 220 mm effective axial FOV. Each ring is composed of 16 block detector, each block with 70×70×20 mm^3 size. For achieving optimized block detector size [14], different calculations and modeling were performed until 70×70 can satisfactorily provide our optimized design. In second design for comparison, cylindrical geometry with the same block detector number and size was simulated to compare with spheroid design performance. The cylindrical model has ring radius of 175 mm and therefore patient bore radius and transaxial FOV in this scanner is 175 mm. All specifications of scanners has illustrated in Table 1.

We used GATE 7.2 Monte Carlo toolkit to simulate both designs [15]. The modeled view of both scanners has shown in Figure 1. Crystal's pixels are 2.3×2.3×20 mm^3 which are placed in 30×30 array in each block. Crystal material for both system is BGO and system electronic response as known "digitizer" in Gate, are exactly the same for both designs.

Table 1: Design characteristics of the spheroid and cylindrical geometry PET scanner.

Specification	Spheroid design	Cylindrical design
Ring diameter (block to block) in mm	398	350
Patient bore in mm	350	350
Number of block detector	48	48
Crystal size (mm)	2.3×2.3×20	2.3×2.3×20
Number of crystals per block(module)	30×30	30×30
Number of transaxial block(module)	16	16
material	BGO	BGO
Number of ring	3	3
Axial FOV (mm)	220	220
Block detector size	70×70×20	70×70×20

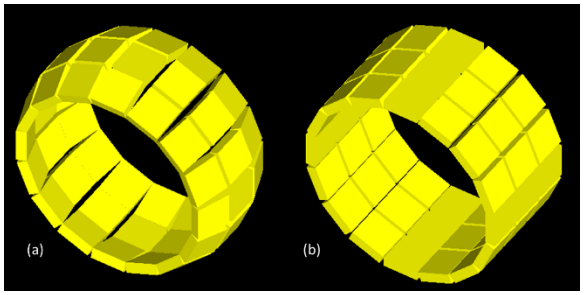

Fig 1. (a) Side view of simulated spheroid geometry PET scanner (b) side view of simulated cylindrical geometry PET scanner.

Detection efficiency estimation

Photon detection efficiency was measured by a 1 MBq gamma back to back photon source stepped at 2.5 cm increments in axial and radial direction. Scatter coincidences were not simulated and maximum ring differences was selected as entire axial FOV. Also no accessories and shielding were simulated in our study because we aimed to focus on comparison study not validation study. The simulations were performed for two energy window 250-750 and 410-613 keV in order to evaluate the effect of tight and loose energy window on scanner detection efficiency.

NEMA sensitivity calculation

According to the NEMA-NU 2007, 700-mm-long plastic tube filled with F-18 along with five concentric aluminum tubes each same 700 mm long with diameter of 6.4, 9.5, 12.7, 15.9 and 19.1 mm were simulated [7, 16]. We selected energy window of 350-700 keV as the average value window and plotted the NEMA sensitivity as a function of the total accumulated aluminum sleeves and the extrapolated to an attenuation-free sensitivity value. This data acquisition was also repeated for cylindrical design.

Analytical estimation of photon detection efficiency

We analytically calculated PDE of both scanners caused by the point source placed in center of FOV. The PDE of a PET scanner is determined by (1) geometric efficiency (*Eg*) which is related to solid angle coverage of the detectors, (2) the intrinsic efficiency (*Ei*) which is related to the crystal material and thickness, crystal packing fraction along with coincidence time and energy window [17] as follows:

$$Photon\ detection\ efficiency\ (PDE) = Ei \times Eg \qquad (1)$$

The total geometric efficiency is given as follows [8, 13]:

$$Eg = \iint_s n \cdot dA/4\pi r^2 \qquad (2)$$

Where dA is finite detector element area which is seen by point source, r is the distance from the point source to the detector surface and n is normal vector of detector surface (Figure 2). For symmetric geometry we estimate the differential solid angle$(d\Omega)$ and integrate these differentials over the entire interior detector surface area of the both cylindrical and spheroid PET systems as follows:

$$Eg = \frac{\sum d\Omega}{4\pi} = \frac{\sum \cos\theta_2\ dA}{4\pi r^2} \qquad (3)$$

$$dA = 4\theta_1 r^2 \sin\theta'_1$$

Where θ_1 $(0 \leqslant \theta_1 < \pi/2)$ and θ'_1 $(0 \leqslant \theta'_1 < \pi/2)$ are the angle in X and Z direction respectively. Because we used square block detector so we would have $\theta_1 = \theta'_1$.

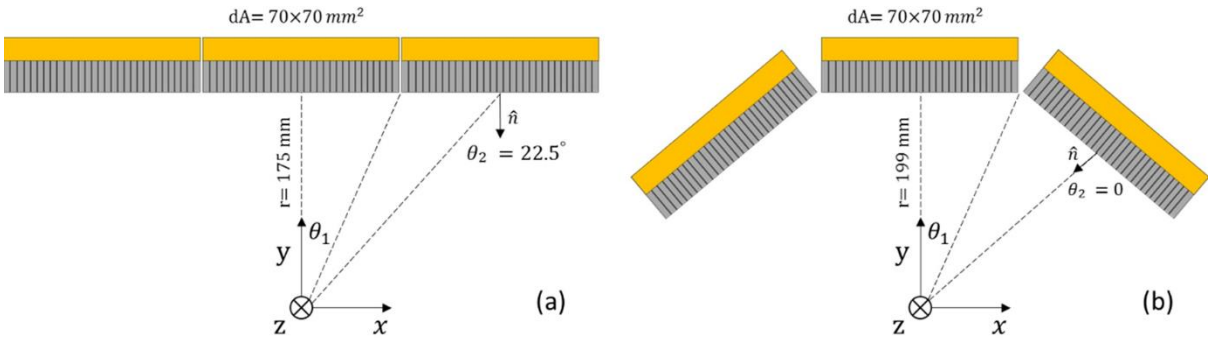

Fig 2. Analytical calculation of differential solid angle coverage of each detector over the entire interior detector surface area of the both (a) cylindrical and (b) spheroid PET systems.

Image reconstruction

For image quality evaluation, we simulated Derenzo phantom composed of spheres with different diameter of 1, 1.25, 1.5, 2, 2.5 mm with activity of 5, 6, 7.5,10 and 12.5 MBq arranged in 5 segments. After simulation, we used STIR3.0 framework to reconstruct obtained projections [18]. Fourier rebinning algorithm (FORE) were applied on simulation output to rebinn projections and then rebinned sinograms were reconstructed using 2D Maximum Likelihood Expectation Maximization (MLEM) algorithm with 15 iterations. A 180×180 image matrix was used with 1.2 mm pixel size. The Smallest spheres in obtained Derenzo image were analyzed to evaluate spheres resolving by 1D line intensity profile as a contrast criteria. To measure system spatial resolution, 3 spheroid sources with diameters of 1 mm and 10 MBq activity were positioned in center of FOV(CFOV) and 9 cm radial offset from CFOV in central slice and 9 cm radial offset and 3 cm axial offset from CFOV. Three-dimensional filtered back projection (FBP3D) algorithm using a ramp filter with a cut-off frequency of 0.5 cm^{-1} used to reconstruct the image and then transaxial, radial and axial spatial resolution were calculated based on fitting Gaussian function to the plotted profiles and measuring of their Full width at half maximum (FWHM).

RESULTS

Detection efficiency

Figure 3 shows the values of PDE in axial and radial direction. In Figure 3a and 3b we observe that PDE is significantly reduced by axial displacement of point source for both scanners in two energy windows. In 250-750 keV, PDE is 21.7% and 23.8% for point source in CFOV for spheroid and cylindrical design respectively. This measurements in 410-613 keV shows 19.5% and 21.3%, therefore we obtained 9.6% and 8.4% PDE increase for cylindrical design in 250-750 and 410-613 keV respectively. In Figure 3c and 3d we see slight changes in PDE value by radial movement of point source, however cylindrical design provides high detection efficiency than spheroid type for different radial positioning of point sources.

NEMA sensitivity

Figure 4 indicates the simulation results of NEMA line source sensitivity measurements in two positions (in center and 7 cm off center), as a function of accumulated aluminum sleeve thickness in a 350-700 keV energy window. We calculated 3.64 kcps/MBq sensitivity for cylindrical type compared with the 3.29 kcps/MBq for spheroid geometry for line source at center. This values increases to 3.78 and 3.23 kcps/MBq for line source at 7-cm offset from center. Therefore, we obtained increment rate in NEMA sensitivity for cylindrical to spheroid design about10.6% (for R= 0) and 17.0 % (for R=7) respectively.

Analytical estimation of photon detection efficiency

According to the equation (3) each detectors solid angles calculated and then sum up the obtained values. For spheroid design the total geometrical efficiency was 46.0% whilst for cylindrical geometry was 55.5%. It should be noted that we selected same intrinsic efficiency for both designs, so geometrical efficiency would be an estimation of the total system detection efficiency.

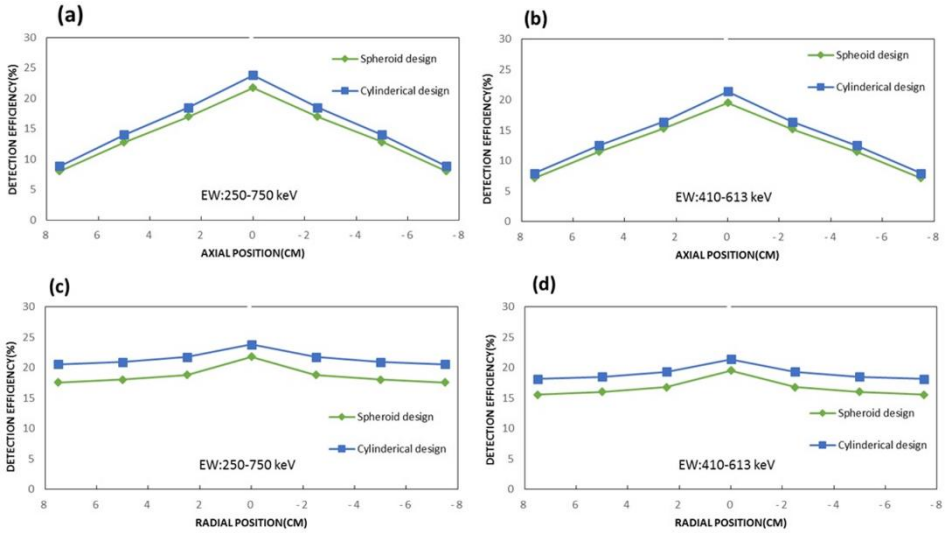

Fig 3. The detection efficiency for both designed scanners were measured with a 1 MBq gamma back to back point source, which stepped at 2.5-cm steps in axial and radial direction in two energy window. (a)Axial direction detection efficiency (250-750 keV). (b) Axial direction detection efficiency (410-613). (c) Radial direction detection efficiency (250-750). (d) Radial direction detection efficiency (410-613).

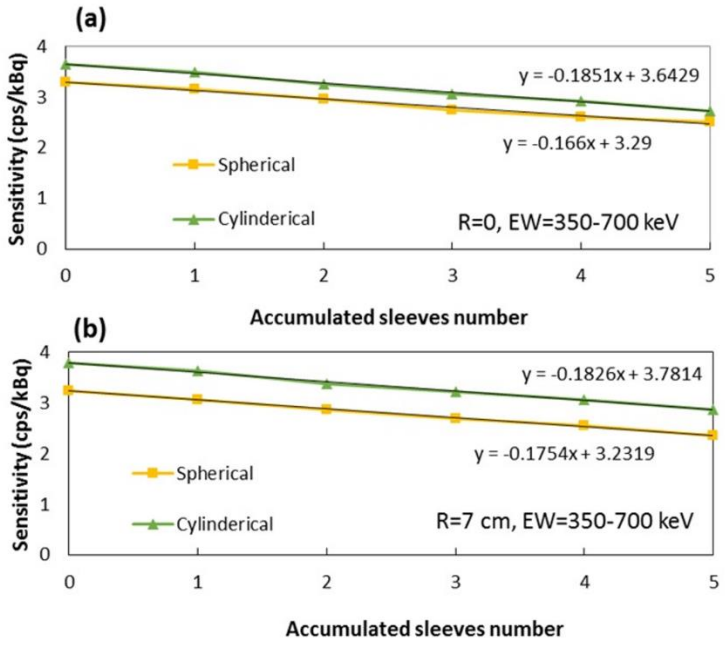

Fig 4. Sensitivity as a function of aluminum sleeve thickness for two modeled scanners using NEMA-2007 line source in (a) R=0 and (b) R=7 cm.

Reconstructed image

Reconstructed Derenzo phantom using FORE+MLEM algorithm for spheroid and cylindrical designs are shown in Figure 5 (a, b).

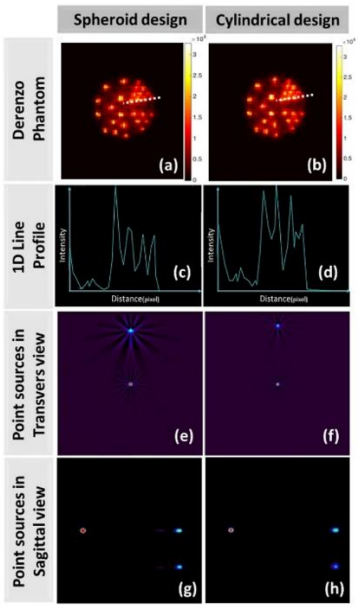

Fig 5. The reconstructed images of Derenzo phantom by FORE+MLEM for spheroid design (a) Cylindrical design (b). 1-D line profile of smallest spheres in Derenzo phantom for spheroid design (c) Cylindrical design (d).The reconstructed image of a point sources by FBP3D in Transverse view for spheroid design (e) Cylindrical design (f). The reconstructed image of a point sources by FBP3D in Sagittal view for spheroid design (g) cylindrical design (h).

We observe that both scanners can resolve all spheres of phantoms. Figure 5 (c, d) show plotted 1-D line profile of the smallest spheres in Derenzo phantom as a contrast criteria with significant peaks and valleys. Also Figure 5 (e, f) indicates transvers view of point sources after FBP3D reconstruction in central slice for both scanners and finally Figure 5 (g, h) shows sagittal view of given point sources.

According to Figure 5 (e-h), the values of spatial resolution (FWHM) calculations for mentioned point sources has listed in Table 2. We noticed the spheroid design has relatively worse spatial resolution than cylindrical geometry for off center point source in transvers direction but can provide better axial resolution especially in axial off center point source.

DISCUSSION

In this study, spheroid PET scanner based on block detector configuration as a candidate for brain imaging was modeled and its performance characteristics evaluated using analytical and Monte Carlo modeling, also results was compared with related and same specification cylindrical PET scanner.

In this study, first of all, photon detection efficiency of point source in axial and radial position in tight and loose energy window were measured by GATE simulation toolkit. Also NEMA sensitivity using line source was calculated for two scanners. Results show that spheroid design provides relatively lower sensitivity than cylindrical PET scanner.

Table 2: Measurements of tangential, radial and axial spatial resolution for different point sources positions within the PET FOV.

FWHM(mm) FBP/MLEM	Spheroid design			Cylindrical Design		
	Tangential	Radial	Axial	Tangential	Radial	Axial
Position 1(cm) (0,0,0)	1.93/1.60	1.80/1.57	1.60/1.56	1.68/1.64	1.94/1.60	1.59/1.58
Position 2 (cm) (0,9,0)	5.70/5.45	4.43/4.21	2.39/2.21	3.83/2.62	4.15/4.04	2.60/2.38
Position 3 (cm) (0,9,3)	3.63/3.57	5.83/3.64	2.97/3.16	3.19/3.30	4.45/4.03	3.69/4.90

Also the results of analytical calculation showed us the cylindrical design provides 9.5 % more efficiency than spheroid design (20% increase ratio) which is compatible with simulations result. Difference in improvement of percentage between analytical and simulation results is due to analytical geometrical efficiency an estimation which were calculated without considering energy and coincidence time window does not explicitly consider scatter and random events [8]. Analytical estimation confirmed our Monte Carlo simulation and indicated that when we want to design a head size compatible spheroid PET based on block detector configuration, we inevitably must increase scanner radius for proper placement of detectors on spheroid surface so this diameter increase degrades the detection efficiency.

According to results of reconstructed images, we found that spatial resolution of off-center sources in spheroid scanner is degraded in transverse plane whilst this scanner provides good spatial resolution with no degradation in CFOV in comparison with cylindrical PET. The spatial resolution degradation of spheroid design can be arise from two factors, the first one is parallax error in transaxial direction caused by peripheral LOR's that interacts obliquely to detectors. The second factor the gap produced between blocks that degrades image quality especially in peripheral source positions. This factor produced a relatively deformed spheres image which has clearly depicted in figure 5e.

Also the results showed spheroid design provides good axial resolution than cylindrical. This is because angled detector in axial direction in spheroid design provides relatively perpendicular angle for emitted photons. The perpendicular angle between detector and emitted photons causes minimal deflection inside of the crystals and deposit their energy by crystals interaction, therefore parallax error would be reduced and axial spatial resolution would be improved. According to the presented explanation, we conclude that spheroid design have less parallax error in axial direction and higher parallax error in transaxial direction in comparison with cylindrical scanner.

In general, this paper is performance evaluation of spheroid design which was not considered as block detector placement drawbacks and the resulted gaps effects in previous studies [10, 13]. We concluded that cylindrical PET scanner has relatively better performance than spheroid design with block detector configuration. Spheroid scanner manufacturing is more complex than cylindrical scanner, therefore we believe cylindrical geometry is one of the best geometries that can provides high quality images. However, for best utilization of spheroid design capability, we propose a new concept in detector manufacturing which prevents LOR's loss and improves system efficiency and image quality by introducing a spheroid fully molded monolithic crystal with no gaps by placing detectors surface to efficiently detect emitted LORs.

For future work, we will further optimize this idea to increase the sensitivity and improve image quality and we will evaluate its performance compared with other brain PET scanners.

CONCLUSION

We have performed analytical and Monte Carlo simulation studies to evaluate performance of the spheroid PET scanner for brain imaging compared to cylindrical design with same detector number and same FOV (Transaxial and axial). Our comparison study indicates that the cylindrical geometry can still provide higher sensitivity (10 % more for NEMA line source).We found that transvers and axial spatial resolution have same value in CFOV for both scanner but for off-center point sources this value is degraded about 0.8 mm FWHM for spheroid design against cylindrical PET. Also spheroid PET based on block detector configuration provides better axial resolution (mean about 0.9 mm FWHM) compared with cylindrical PET in off-center point sources.

Acknowledgment

This work was supported under grant number 28203, Tehran University of Medical Sciences, Tehran, Iran.

REFERENCES

1. Zaidi H, Montandon ML. The new challenges of brain PET imaging technology. Curr Med Imaging Rev. 2006 Feb 1;2(1):3-13.
2. Gong K, Majewski S, Kinahan PE, Harrison RL, Elston BF, Manjeshwar R, Dolinsky S, Stolin AV, Brefczynski-Lewis JA, Qi J. Designing a compact high performance brain PET scanner-simulation study. Phys Med Biol. 2016 May 21;61(10):3681-97.
3. González AJ, Majewski S, Sánchez F, Aussenhofer S, Aguilar A, Conde P, Hernández L, Vidal LF, Pani R, Bettiol M, Fabbri A, Bert J, Visvikis D, Jackson C, Murphy J, O'Neill K, Benllocha JM. The MINDView brain PET detector, feasibility study based on SiPM arrays. Nucl Instrum Methods Phys Res A. 2016 May 11;818:82-90.
4. Herzog H, Langen KJ, Weirich C, Rota Kops E, Kaffanke J, Tellmann L, Scheins J, Neuner I, Stoffels G, Fischer K, Caldeira L, Coenen HH, Shah NJ. High resolution BrainPET combined with simultaneous MRI. Nuklearmedizin. 2011;50(2):74-82.
5. Bowen SL, Wu Y, Chaudhari AJ, Fu L, Packard NJ, Burkett GW, Yang K, Lindfors KK, Shelton DK, Hagge R, Borowsky AD, Martinez SR, Qi J, Boone JM, Cherry SR, Badawi RD. Initial characterization of a dedicated breast PET/CT scanner during human imaging. J Nucl Med. 2009 Sep;50(9):1401-8.
6. Moliner L, Gonzalez AJ, Soriano A, Sanchez F, Correcher C, Orero A, Carles M, Vidal LF, Barbera J, Caballero L, Seimetz M, Vazquez C, Benlloch JM. Design and evaluation of the MAMMI dedicated breast PET. Med Phys. 2012 Sep;39(9):5393-404.
7. Sheikhzadeh P, Sabet H, Ghadiri H, Geramifar P, Mahani H, Ghafarian P, Ay MR. Development and validation of an accurate GATE model for NeuroPET scanner. Phys Med. 2017 Aug;40:59-65.
8. Habte F, Foudray AM, Olcott PD, Levin CS. Effects of system geometry and other physical factors on photon sensitivity of high-resolution positron emission tomography. Phys Med Biol. 2007 Jul 7;52(13):3753-72.
9. Ficke DC, Hood JT, Ter-Pogossian MM. A spheroid positron emission tomograph for brain imaging: a feasibility study. J Nucl Med. 1996 Jul;37(7):1219-25.
10. Moghaddam NM, Karimian A, Mostajaboddavati SM, Vondervoort E, Sossi V. Preliminary design and simulation of a spherical brain PET system (SBPET) with liquid xenon as scintillator. Nukleonika. 2009;54(1):33-8.
11. Sheikhzadeh P, Sabet H, Ghadiri H, Ghafarian P, Ay M. Design and performance evaluation of a novel brain PET geometry based on partial cylindrical detector using Monte Carlo simulation. Eur J Nucl Med Mol Imaging. 2016;43(suppl 1):S94.
12. Cho ZH, Kim YS, Hilal SK, Kim YH. New spherical PET design with Fresnel aperture orientation. Int J Imag Syst Tech. 1989 Sep 1;1(2):196-206.
13. Tashima H, Yamaya T. Proposed helmet PET geometries with add-on detectors for high sensitivity brain imaging. Phys Med Biol. 2016 Oct 7;61(19):7205-7220.
14. Mahani H, Raisali G, Kamali-Asl A, Ay MR. Monte Carlo optimization of crystal configuration for pixelated molecular SPECT scanners. Nucl Instrum Methods Phys Res A. 2017 Feb 1;844:1-6.
15. Jan S, Santin G, Strul D, Staelens S, Assié K, Autret D, Avner S, Barbier R, Bardiès M, Bloomfield PM, Brasse D, Breton V, Bruyndonckx P, Buvat I, Chatziioannou AF, Choi Y, Chung YH, Comtat C, Donnarieix D, Ferrer L, Glick SJ, Groiselle CJ, Guez D, Honore PF, Kerhoas-Cavata S, Kirov AS, Kohli V, Koole M, Krieguer M, van der Laan DJ, Lamare F, Largeron G, Lartizien C, Lazaro D, Maas MC, Maigne L, Mayet F, Melot F, Merheb C, Pennacchio E, Perez J, Pietrzyk U, Rannou FR, Rey M, Schaart DR, Schmidtlein CR, Simon L, Song TY, Vieira JM, Visvikis D, Van de Walle R, Wieërs E, Morel C. GATE: a simulation toolkit for PET and SPECT. Phys Med Biol. 2004 Oct 7;49(19):4543-61.
16. National Electrical Manufacturers Association. NEMA Standards Publication NU 2-2007. Performance measurements of positron emission tomographs. 2007.
17. Cherry S.R., Dahlbom M. PET: Physics, Instrumentation, and Scanners. In: PET. New York: Springer; 2004.
18. Thielemans K, Tsoumpas C, Mustafovic S, Beisel T, Aguiar P, Dikaios N, Jacobson MW. STIR: software for tomographic image reconstruction release 2. Phys Med Biol. 2012 Feb 21;57(4):867-83.